Applied Mathematical Sciences, Vol. 4, 2010, no. 13, 643 - 655

Radiation Effects on Natural Convection MHD Flow in a Rotating Vertical Porous Channel Partially Filled with a Porous Medium

Dileep Singh Chauhan and Priyanka Rastogi

Department of Mathematics, University of Rajasthan
Jaipur-302055, India
dileepschauhan@yahoo.com

Abstract

The unsteady natural convection MHD flow of a rotating viscous electrically conducting fluid in a vertical channel partially filled by a porous medium with high porosity in the presence of radiation effects, has been investigated. It is assumed that the conducting fluid is gray, emitting-absorbing radiation, and non-scattering medium. The two infinite vertical porous plates of the channel are subjected to a constant injection velocity at the one plate and the same constant suction velocity at the other plate. The entire system rotates about the axis normal to the plates with a uniform angular velocity. The analytic expressions for velocity and temperature field are obtained and effects of the radiation-conduction parameter (Stark number), Prandtl number, Grashof number, rotation parameter, magnetic field, and permeability of the porous medium on the velocity field, temperature field and Nusselt number have been discussed in the analysis.

Keywords: Natural convection, radiation, permeability, MHD, rotating, porous medium

1. Introduction

Channels are frequently used in various applications in designing ventilating and heating of buildings, cooling electronic components, drying several types of agriculture products grain and food, and packed bed thermal storage. Convective flows in channels driven by temperature differences of

bounding walls have been studied and reported, extensively in literature. Free convection flows in vertical slots were discussed by Aung et al. (1972), Burch et al. (1985), Kim et al. (1990), Buhler (2003), Weidman (2006), Magyari (2007), Weidman and Medina (2008).

Radiative convective flows are frequently encountered in many scientific and environmental processes, such as astrophysical flows, water evaporation from open reservoirs, heating and cooling of chambers, and solar power technology. Several researchers have investigated radiative effects on heat transfer in non-porous and porous medium utilizing the Rosseland or other radiative flux model, such as Raptis (1998), Hall et al. (1999), Hakiem (2000), Raptis (2001), Bakier (2001), Raptis and Perdikis (2004), Sanyal and Adhikari (2006), Rao (2007), Prasad and Reddy (2008).

Magnetohydrodynamics deals with dynamics of an electrically conducting fluid, which interacts with a magnetic field. The study of heat transfer and flow, through and across porous media, is of great theoretical interest because it has been applied to a variety of geophysical and astrophysical phenomena. Practical interest of such study includes applications in electromagnetic lubrication, boundary cooling, bio-physical systems and in many branches of engineering and science. Extensive research in this discipline has been reported such as Alchaar et al. (1995), Bian et al. (1996), Yih (1998), Geindreau and Auriault (2002), Chauhan and Jain (2005), Hayat et al. (2008), Kandasamy et al. (2009).

Extensive research work has been carried out in recent years to study the effects of various solid matrix and fluid flow parameters on the free convection in channels partially filled by porous materials. Beckermann et al. (1987) examined free convection flow between a fluid and a porous layer in a rectangular enclosure. Convection effects are investigated in an inclined channel with porous substrates at the bounding rigid walls by Chauhan and Soni (1994). Mixed convection was studied by Chang and Chang (1996) in a vertical channel partially filled with highly permeable porous media. Al-Nimr and Hadded (1999) examined the effects of free convection fully developed flow through open-ended vertical channels that are filled partially by porous medium. Alkam et al. (2002) examined forced convection in such channels. Al-Nimr and Khadrawi (2003) investigated transient free convection flow in channels partially filled by porous substrates in various configurations.

The studies in convection flows of a viscous electrically conducting fluid in rotating channels partially filled with porous substrates in the presence of a magnetic field have a wide range of scientific and engineering applications. During alloy solidification convection effects are important because they affect the solid fluid content within a porous layer known as mushy layer. Further, these rotating flows are electromagnetically braked by a force (Lorentz force) and therefore have applications, e.g. in Nuclear engineering [Mc Whirter et al., (1998)], in metallurgy-during the solidification process [(Prescott and Incropera, (1993), Riahi (2002)], and in many fluid engineering applications.

In the present paper, the objective is to investigate the effects of radiation, magnetic field, permeability of the porous substrate and injection-suction on the unsteady free convective MHD flow in vertical channel partially filled with a porous substrate when the entire system rotates about an axis normal to the

channel plates. The Rosseland radiation flux model is employed which gives good simulating results for optically thick fluids which are absorbing, emitting, gray but not scattering.

2. Formulation of the problem

We consider the unsteady MHD free convective flow in a vertical parallel porous plate channel partially filled with a porous material and partially with a clear electrically conducting fluid. The entire system rotates about the axis normal to the plates with uniform angular velocity Ω. The channel is of width ' d ' and the thickness of the porous medium is ' h '. A cartesian coordinate system is assumed and z-axis is taken normal to the plates while x and y axes, respectively are in the upward and perpendicular directions on the plate $z = 0$. Two vertical plates are situated at $z = 0$ and $z = d$. The origin is taken at the plate, $z = 0$ and the channel is oriented vertically upward along x-axis. Plates are infinite in extent in x and y directions. These plates are subjected to a constant injection velocity (w_0) at one plate $(z = 0)$ and the same constant suction velocity (w_0) at the other plate $(z = d)$. A uniform magnetic field B_0 is applied along an axis normal to the plates (z-axis) and the entire system rotates about this axis. It is assumed that the magnetic Reynolds number is very small, so that induced magnetic field is neglected [Cowling (1957)].

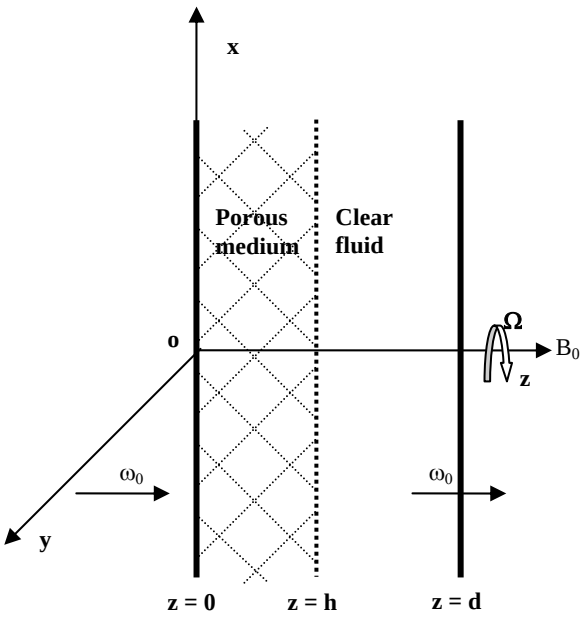

Fig.1 Schematic diagram

We denote the velocity components $\bar{u}, \bar{v}, \bar{w}$ in porous medium region, and u', v', w' in clear fluid region, in the x, y, z directions respectively. $\bar{T}$ denotes temperature in the porous region, T' denotes temperature in the clear fluid region, and t' denotes time. Since the channel plates are infinite in extent, velocity and temperature components depend only on z' and t', and further, the continuity equation gives $\bar{w} = w' = w_0$ (constant).

The fluid considered here is assumed to be gray, emitting-absorbing radiation but a non-scattering medium. It is also assumed that there is radiation

only from the fluid. Further it is assumed that the thermal radiation is present in the form of a unidirectional flux, transverse to the vertical plates, and to describe the thermal radiative heat transfer, the Rosseland approximation is used in the energy equation. Further, the fluid and the porous structure are assumed to be in local thermal equilibrium, and all the fluid properties are assumed to be constant except that the influence of the density variation with temperature is considered only in the body force term.

Using Rosseland approximation, the radiative heat transfer takes the form following Siegel and Howell (1972), respectively in clear fluid and porous region as follows:

$$q_r = -\frac{4\sigma^*}{3K^*}\frac{\partial T'^4}{\partial z'}; \qquad \bar{q}_r = -\frac{4\sigma^*}{3K^*}\frac{\partial \bar{T}^4}{\partial z'}. \tag{1}$$

where, σ^* is Stefan-Boltzmann constant and K^* is mean absorption coefficient for thermal radiation.

Following Raptis (1998) the temperature functions in (1) can be expressed as a linear function of temperature. Expanding T'^4 and $\bar{T}^4$ in a Taylor series about T_d (constant temperature of the right wall) and neglecting higher-order terms, we obtain

$$T'^4 = 4T_d^{\,3}T' - 3T_d^{\,4} \text{ , and } \bar{T}^4 = 4T_d^{\,3}\bar{T} - 3T_d^{\,4}. \tag{2}$$

By introducing the following non-dimensional quantities,

$$\eta = \frac{z'}{d},\ \alpha = \frac{h}{d},\ K = \frac{K'}{d^2},\ \lambda = \frac{w_0 d}{\upsilon},\ t = \frac{\upsilon t'}{d^2},\ n = \frac{d^2 n'}{\upsilon},$$

$$U = \frac{\bar{u}}{w_0},\ V = \frac{\bar{v}}{w_0},\ u = \frac{u'}{w_0},\ v = \frac{v'}{w_0},\ \theta = \frac{\bar{T} - T_d}{T_0 - T_d},\ T = \frac{T' - T_d}{T_0 - T_d},$$

and using eqs. (1) and (2), the dimensionless governing equations in the porous medium region - I $(0 \le \eta \le \alpha)$ and the clear fluid region – II $(\alpha \le \eta \le 1)$ for the MHD convective flow of a radiative fluid in the rotating system are respectively given by

For porous region - I

$$\frac{\partial U}{\partial t} + \lambda\frac{\partial U}{\partial \eta} - 2\,\mathrm{Re}\,V = \frac{\partial^2 U}{\partial \eta^2} + \mathrm{Gr}(\theta - 1) - \frac{U}{K} - M^2 U, \tag{3}$$

$$\frac{\partial V}{\partial t} + \lambda\frac{\partial V}{\partial \eta} + 2\,\mathrm{Re}\,V = \frac{\partial^2 V}{\partial \eta^2} - \frac{V}{K} - M^2 V, \tag{4}$$

$$\frac{\partial \theta}{\partial t} + \lambda\frac{\partial \theta}{\partial \eta} = \left(\frac{3N+4}{3N\,\mathrm{Pr}}\right)\frac{\partial^2 \theta}{\partial \eta^2}. \tag{5}$$

For clear fluid region – II

$$\frac{\partial u}{\partial t} + \lambda\frac{\partial u}{\partial \eta} - 2\,\mathrm{Re}\,v = \frac{\partial^2 u}{\partial \eta^2} + \mathrm{Gr}(T - 1) - M^2 u, \tag{6}$$

$$\frac{\partial v}{\partial t} + \lambda\frac{\partial v}{\partial \eta} + 2\,\mathrm{Re}\,u = \frac{\partial^2 v}{\partial \eta^2} - M^2 v, \tag{7}$$

$$\frac{\partial T}{\partial t}+\lambda\frac{\partial T}{\partial \eta}=\left(\frac{3N+4}{3N\,Pr}\right)\frac{\partial^2 T}{\partial \eta^2}, \tag{8}$$

where, $Re=\dfrac{\Omega d^2}{\upsilon}$, $Pr=\dfrac{\mu C_p}{k}$, $N=\dfrac{k\,K^*}{4\sigma^* T_d^{\,3}}$, $M^2=\dfrac{\sigma}{\mu}B_0{}^2 d^2$, $Gr=\dfrac{g\,\beta\left(T_0-T_d\right)d^2}{\upsilon w_0}$.

Here, $\rho, \upsilon, \beta, \sigma, k, C_p, g, n'$ denote density, kinematic viscosity, coefficient of volume expansion, electrical conductivity, thermal conductivity, specific heat at constant pressure, acceleration due to gravity and dimensional scalar constant respectively. K' is the dimensional permeability of the porous medium, K is the dimensionless permeability of the porous medium , T_0 is a reference temperature and T_d is constant temperature of the right wall.

The corresponding boundary conditions in non-dimensional form are given by

$$\begin{aligned}
&\text{at } \eta=0; && U=V=0, && \theta=1+\varepsilon e^{nt},\\
&\text{at } \eta=\alpha; && U=u, && V=v, && \theta=T,\\
& && \frac{\partial U}{\partial \eta}=\frac{\partial u}{\partial \eta}, && \frac{\partial V}{\partial \eta}=\frac{\partial v}{\partial \eta}, && \frac{\partial \theta}{\partial \eta}=\frac{\partial T}{\partial \eta},\\
&\text{at } \eta=1; && u=v=0, && T=0.
\end{aligned} \tag{9}$$

Here, $\varepsilon<<1$ (a positive constant), and n is a dimensionless scalar constant.

3. Method of solution

We first solve eqs. (5) and (8) for temperature distribution in porous and clear fluid region. Let us assume

$$\theta(\eta,t)=\theta_0(\eta)+\varepsilon\,\theta_1(\eta)e^{nt} \tag{10}$$

and $$T(\eta,t)=T_0(\eta)+\varepsilon\,T_1(\eta)e^{nt} \tag{11}$$

Substituting (10) and (11) in eqs. (5) and (8) and the corresponding boundary conditions for the temperature distribution, and comparing the coefficients of e^{nt}, we obtain

$$\frac{\partial^2\theta_0}{\partial\eta^2}-\left(\frac{3\lambda N\,Pr}{3N+4}\right)\frac{\partial\theta_0}{\partial\eta}=0, \tag{12}$$

$$\frac{\partial^2\theta_1}{\partial\eta^2}-\left(\frac{3\lambda N\,Pr}{3N+4}\right)\frac{\partial\theta_1}{\partial\eta}-\left(\frac{3nN\,Pr}{3N+4}\right)\theta_1=0, \tag{13}$$

$$\frac{\partial^2 T_0}{\partial\eta^2}-\left(\frac{3\lambda N\,Pr}{3N+4}\right)\frac{\partial T_0}{\partial\eta}=0, \tag{14}$$

$$\frac{\partial^2 T_1}{\partial\eta^2}-\left(\frac{3\lambda N\,Pr}{3N+4}\right)\frac{\partial T_1}{\partial\eta}-\left(\frac{3nN\,Pr}{3N+4}\right)T_1=0, \tag{15}$$

and the corresponding boundary conditions:

at $\eta = 0$; $\theta_0 = 1,\ \theta_1 = 1,$

at $\eta = \alpha$; $\theta_0 = T_0,\ \theta_1 = T_1,\ \dfrac{\partial\theta_0}{\partial\eta} = \dfrac{\partial T_0}{\partial\eta},\ \dfrac{\partial\theta_1}{\partial\eta} = \dfrac{\partial T_1}{\partial\eta},$

at $\eta = 1$; $T_0 = 0,\ T_1 = 0.$ (16)

On solving (12)-(16), we obtain

$$\theta_0 = \frac{e^{a_1\eta} - e^{a_1}}{1 - e^{a_1}} \text{ and } \theta_1 = \frac{e^{a_3+a_4\eta} - e^{a_3\eta+a_4}}{e^{a_3} - e^{a_4}} \tag{17}$$

$$T_0 = \frac{e^{a_1\eta} - e^{a_1}}{1 - e^{a_1}} \text{ and } T_1 = \frac{e^{a_3+a_4\eta} - e^{a_3\eta+a_4}}{e^{a_3} - e^{a_4}} \tag{18}$$

where, $a_1 = \dfrac{3\lambda N\,\mathrm{Pr}}{3N+4}$, $a_2 = \dfrac{3nN\,\mathrm{Pr}}{3N+4}$, $a_3 = \dfrac{a_1 + \sqrt{a_1^{\,2} + 4a_2}}{2}$, $a_4 = \dfrac{a_1 - \sqrt{a_1^{\,2} + 4a_2}}{2}$.

The non-dimensional rate of heat transfer (Nusselt number) at $\eta = 0$ is given by

$$\mathrm{Nu}_0 = \left(\frac{\partial\theta}{\partial\eta}\right)_{\eta=0} = \left(\frac{a_1}{1-e^{a_1}}\right) + \varepsilon\, e^{nt}\left(\frac{a_4 e^{a_3} - a_3 e^{a_4}}{e^{a_3} - e^{a_4}}\right) \tag{19}$$

The non-dimensional rate of heat transfer (Nusselt number) at $\eta = 1$ is given by

$$\mathrm{Nu}_1 = \left(\frac{\partial T}{\partial\eta}\right)_{\eta=1} = \left(\frac{a_1 e^{a_1}}{1-e^{a_1}}\right) + \varepsilon\, e^{nt+a_3+a_4}\left(\frac{a_4 - a_3}{e^{a_3} - e^{a_4}}\right) \tag{20}$$

Velocity distribution

Let $\bar{F} = U + iV$, and $F = u + iv$ (21)

Using above, and the boundary conditions, eqs. (3-4) and (6-7) reduce to

$$\frac{\partial\bar{F}}{\partial t} + \lambda\frac{\partial\bar{F}}{\partial\eta} + 2i\,\mathrm{Re}\,\bar{F} = \frac{\partial^2\bar{F}}{\partial\eta^2} + \mathrm{Gr}(\theta - 1) - \left(\frac{1}{K} + M^2\right)\bar{F} \tag{22}$$

$$\frac{\partial F}{\partial t} + \lambda\frac{\partial F}{\partial\eta} + 2i\,\mathrm{Re}\,F = \frac{\partial^2 F}{\partial\eta^2} + \mathrm{Gr}(T - 1) - M^2 F \tag{23}$$

and the corresponding boundary conditions are given by

at $\eta = 0$; $\bar{F} = 0,$

at $\eta = \alpha$; $\bar{F} = F,\ \dfrac{\partial\bar{F}}{\partial\eta} = \dfrac{\partial F}{\partial\eta},$

at $\eta = 1$; $F = 0.$ (24)

Now, let us assume that

$$U(\eta, t) = U_0(\eta) + \varepsilon\, U_1(\eta)e^{nt}$$

$$V(\eta, t) = V_0(\eta) + \varepsilon\, V_1(\eta)e^{nt}$$

$$u(\eta, t) = u_0(\eta) + \varepsilon\, u_1(\eta)e^{nt}$$

$$v(\eta, t) = v_0(\eta) + \varepsilon\, v_1(\eta)e^{nt}$$

so that $\bar{F}(\eta, t) = U_0(\eta) + iV_0(\eta) + \varepsilon\left[U_1(\eta) + iV_1(\eta)\right]e^{nt}$

$$= \bar{F}_0(\eta) + \varepsilon\bar{F}_1(\eta)e^{nt}$$

$$F(\eta,t) = u_0(\eta) + iv_0(\eta) + \varepsilon\left[u_1(\eta) + iv_1(\eta)\right]e^{nt}$$
$$= F_0(\eta) + \varepsilon F_1(\eta)e^{nt} \quad (25)$$

Substituting (25) in (22-24) and comparing the coefficients of e^{nt}, we obtain

$$\frac{\partial^2\overline{F}_0}{\partial\eta^2} - \lambda\frac{\partial\overline{F}_0}{\partial\eta} - b_3\overline{F}_0 + Gr(\theta_0 - 1) = 0 \quad (26)$$

$$\frac{\partial^2\overline{F}_1}{\partial\eta^2} - \lambda\frac{\partial\overline{F}_1}{\partial\eta} - b_4\overline{F}_1 + Gr\theta_1 = 0 \quad (27)$$

$$\frac{\partial^2 F_0}{\partial\eta^2} - \lambda\frac{\partial F_0}{\partial\eta} - b_1 F_0 + Gr(T_0 - 1) = 0 \quad (28)$$

$$\frac{\partial^2 F_1}{\partial\eta^2} - \lambda\frac{\partial F_1}{\partial\eta} - b_2 F_1 + GrT_1 = 0 \quad (29)$$

and the corresponding boundary conditions:

at $\eta = 0$; $\quad \overline{F}_0 = 0, \quad \overline{F}_1 = 0,$

at $\eta = \alpha$; $\quad \overline{F}_0 = F_0, \quad \overline{F}_1 = F_1,$

$$\frac{\partial\overline{F}_0}{\partial\eta} = \frac{\partial F_0}{\partial\eta}, \quad \frac{\partial\overline{F}_1}{\partial\eta} = \frac{\partial F_1}{\partial\eta},$$

at $\eta = 1$; $\quad F_0 = 0, \quad F_1 = 0.$ (30)

where, $b_1 = M^2 + 2i\,Re, \quad b_2 = M^2 + n + 2i\,Re,$

$$b_3 = \frac{1}{K} + M^2 + 2i\,Re, \quad b_4 = \frac{1}{K} + M^2 + n + 2i\,Re.$$

On solving (26)-(29), we get

$$\overline{F}_0 = B_5 e^{b_{13}\eta} + B_6 e^{b_{14}\eta} - b_{15}e^{a_1\eta} - b_{16} \quad (31)$$

$$\overline{F}_1 = B_7 e^{b_{17}\eta} + B_8 e^{b_{18}\eta} - b_{19}e^{a_4\eta} + b_{20}e^{a_3\eta} \quad (32)$$

$$F_0 = B_1 e^{b_5\eta} + B_2 e^{b_6\eta} - b_7 e^{a_1\eta} - b_8 \quad (33)$$

$$F_1 = B_3 e^{b_9\eta} + B_4 e^{b_{10}\eta} - b_{11}e^{a_4\eta} + b_{12}e^{a_3\eta} \quad (34)$$

Where, $B_1, B_2, B_3, B_4, B_5, B_6, B_7, B_8$ are constants of integration that are determined by the boundary conditions (30), and these constants of integration and other constants are not reported here for the sake of brevity.

Discussions

This study considers the configuration in vertical parallel plate channel where a porous substrate is perfectly attached to the left vertical plate. The effects of various parameters on the thermal and hydrodynamic behaviors of buoyancy induced flow in rotating vertical channel are studied. The results are presented graphically and discussed. Interest in such type of work in a rotating frame, is motivated by its importance in several practical situations, and such study has some relevance in metallurgy where the process of solidification is characterized

by the presence of a liquid, a mushy zone and a solid zone; in geothermal systems; cooling of electronic components; and in many fluid engineering applications.

Figures 2-9 illustrates the effects of various parameters, such as thermal Grashof number Gr, permeability parameter K, Stark number N, magnetic parameter M^2, rotation parameter Re, Prandtl number Pr, injection-suction parameter λ, and temporal parameter t, on the primary and secondary flow in the channel. Temperature of the heated wall (left) at $z = 0$ is a function of time, as given by in the boundary conditions, and the cooled wall at $z = d$ is maintained at a constant temperature. Further it is assumed that the temperature difference is sufficiently small, so that the density changes of the fluid in the system will be small. When the injection-suction parameter λ is positive, fluid is injected through the hot wall into the channel and sucked out through the cold wall. We observed in Figs. 2-6 that because of the temperature gradient in the system, the fluid near the left wall (hot wall) rises in the attached porous substrate and in the nearby region of the fluid-porous interface, and near the cold wall it descends. The motion of the fluid in the x-direction is a result of the buoyant force term in the momentum equation. In Fig. 2, we observe that this rise and fall of the fluid in the channel is further enhanced by the rise in the thermal Grashof number Gr. It is also seen in Fig. 3 that the velocity profiles in x-direction (primary flow) increases in the porous region and the nearby fluid-porous interface in the channel by increasing the permeability parameter K. However, its magnitude decreases in the middle and the effect of K is insignificant near the other wall at $z = d$. It is so because the Darcian drag force in the attached porous substrate to the left wall, is inversely proportional to K so that with the rise in K, the porous medium impedance is reduced and thus the flow is accelerated in it.

Influence of Prandtl number on the primary flow is illustrated in Fig.4, keeping all other parameters fixed. It explains the relative effectiveness of momentum diffusion and thermal diffusion in the fluid flow. Fluids with low Pr value correspond to low density gases and denser fluids are associated with higher Pr value. For values of Pr less than unity, e.g. 0.1, 0.71, as in Fig.4, the heat will diffuse faster than the momentum causing a decrease in the magnitude of velocity. For values of Pr greater than unity, e.g.5, 7, 10, 15, 100 the momentum will diffuse faster than the heat in flow leading to an increase in velocity. It is observed that by increasing Pr, the primary flow increases in the porous substrate attached to the left hot wall and its nearby region, whereas its magnitude decreases near the other wall. For higher Pr values, primary flow increases throughout in the channel.

In Fig. 5 we see that keeping other parameters fixed, by increasing the magnetic parameter M^2, the primary velocity which is positive in the porous medium and nearby region decreases since a resistive force (Lorentz force) acts against the flow and tends to slow down velocity flow field in this region whereas it accelerates in the remaining channel in the negative direction. The effect of thermal radiation can be explained through the Stark number N, which is defined as relative contribution of the conduction heat transfer to the thermal radiation transfer. Thus with smaller N values, the thermal radiation is larger than the thermal conduction. It is seen in Fig. 5 that by increasing N the primary flow

increases near the left wall in the porous medium and it's near by region but its magnitude decreases in the region near the other wall. Similar results are observed in Fig. 6 with the parameters Re, λ, t.

Figures 2-6 reveal that η (non-dimensional z coordinate) in the channel, where the primary flow becomes zero and then changes sign, is increased with the increase in $K, N, \mathrm{Pr}, \mathrm{Re}, \lambda, t$ and decreases in M^2. However this point is unaffected by the variation of the thermal Grashof number Gr.

Figures 7-9 illustrate the secondary velocity profiles for various values of the parameters. Since the vertical channel is rotating uniformly about an axis normal to it, i.e. about z-axis, secondary flow is generated in y-direction. When the rotation parameter Re is small it accelerates the secondary velocity component in the channel, however when Re is large it still increases this flow in the right part of the channel but it retards near the left wall in porous medium and its nearby region. When rotation parameter Re is small, permeability of the porous medium K enhances the secondary flow in the channel, however when Re is large, K enhances the secondary flow near the left wall but it retards in the middle. Grashof number Gr also enhances it. As time progresses secondary flow decelerates. The effect of the parameter M^2 or N or Pr or λ, is to retard the secondary flow in the channel.

Additionally, plots of temperature profiles and dimensionless rate of heat transfer (Nusselt number) have been computed versus η (non-dimensional z-coordinate) and Stark number N, respectively, and illustrated in Figs. 10-12. When the parameter λ is negative, fluid is sucked out from the left hot wall and injected into the channel through the right cold wall. Comparing the profile curves in Fig. 10, it is found that the Prandtl number Pr reduces the temperature in the channel. Similarly, an increase in N, i.e. decrease in thermal radiation flux, also serves to decrease temperature in the channel. However, when the parameter λ is positive, i.e. when the fluid is injected into the channel through the left hot wall and sucked out through the other wall, the above effects are reversed. In Fig. 10, it is also observed that by increasing λ from a negative value to a positive value temperature in the channel rises, and also as time t progresses.

Figs. 11 and 12 illustrate the variations of the Nusselt number at the hot wall, Nu_0 and at the cold wall Nu_1. It is found that Nu_0 at the hot wall $(\eta = 0)$ decreases in magnitude by increasing the radiation-conduction parameter N or Prandtl number Pr when the parameter λ is positive. When λ is negative, Nu_0 increases in magnitude with the rise in N or Pr. However, keeping Pr fixed and changing λ from negative value to positive, Nu_0 decreases for all N. Exactly reverse results are observed for the Nusselt number Nu_1 at the cold wall $(\eta = 1)$.

Acknowledgement

The support provided by the University Grants Commission through Junior Research Fellowship to one of the authors Ms. Priyanka Rastogi, is gratefully acknowledged.

References

[1] A. Raptis, Radiation and free convection flow through a porous medium, Int. Commun. Heat Mass Transf., 25(1998), 289-295.
[2] A. Raptis, Radiation and flow through a porous medium, J. Porous Media, 4(2001), 271-273.
[3] A. Raptis and C. Perdikis, Unsteady flow through a highly porous medium in the presence of radiation, Transport in Porous Media, 57(2004), 171-179.
[4] A.Y. Bakier, Thermal radiation effects on mixed convection from vertical surfaces in saturated porous media, Int. Comm. Heat and Mass Transfer, 28(2001), 243-248.
[5] C. Beckermann, S. Ramadhyani, and R. Viskanta, Natural convection flow and heat transfer between a fluid layer and a porous layer inside a rectangular enclosure, J. Heat Transf., 109(1987), 363-370.
[6] C.G. Rao, Interaction of surface radiation with conduction and convection from a vertical channel with multiple discrete heat sources in the left wall, Numer. Heat Transfer Part A : Appl., 52(2007), 831-848.
[7] C. Geindreau and J.L. Auriault, Magnetohydrodynamic flows in porous media, J. Fluid. Mech., 466(2002), 343-363.
[8] D.C. Sanyal and A. Adhikari, Effects of radiation on MHD vertical channel flow, Bull. Cal. Math. Soc., 98, 5(2006), 487-497.
[9] D. Hall, G.C. Vliet and T.L. Bergman, Natural convection cooling of vertical rectangular channels in air considering radiation and wall conduction, J. Electron. Pack., 121(1999), 75-84.
[10] D.N. Riahi, Effects of rotation on convection in a porous layer during alloy solidification. In Transport phenomena in porous media II (eds.) D.B. Ingham and I. Pop, Pergamon, Oxford, 2002, pp.316-340.
[11] D.S. Chauhan and V. Soni, Convection effects in an inclined channel with highly permeable layers, Arch. Mech., 46, 3(1994), 399-406.
[12] D.S. Chauhan and R. Jain, Three dimensional MHD steady flow of a viscous incompressible fluid over a highly porous layer, Modelling, Measurement and Control B, 74, 5(2005), 19-34.
[13] EI.M.A. Hakiem, MHD oscillatory flow on free convection radiation through a porous medium with constant suction velocity, J. Magnetism and Magnetic Materials, 220(2000), 271-276.
[14] E. Magyari, Normal mode analysis of the fully developed free convection flow in a vertical slot with open to capped ends, Heat Mass Transf., 43(2007), 827-832.
[15] J. Mc Whirter, M. Crawford, D. Klein, and T. Sanders, Model for inertia less magnetohydrodynamic flow in packed beds, Fusion Technol., 33(1998), 22-30.
[16] K.A. Yih, The effect of uniform suction/blowing on heat transfer of magnetohydrodynamic Hiemenz flow through porous media, Acta Mechanica, 130(1998) 147-158.
[17] K. Buhler, Special solutions of the Boussinesq-equations for free convection flows in a vertical gap, Heat Mass Transf., 39(2003), 631-638.
[18] M.A. Al-Nimr and A.F. Khadrawi, Transient free convection fluid flow in domains partially filled with porous media, Transport in porous media, 51(2003), 157-172.
[19] M.A. Al-Nimr and O.H. Haddad, Fully developed free convection in open-ended vertical channels partially filled with porous material, J. Porous Media, 2(1999), 179-189.
[20] M.K. Alkam, M.A. Al-Nimr, M.O. Hamdan, On forced convection in channels partially filled with porous substrates, Heat and Mass Transf., 38(2002), 337-342.
[21] P.D. Weidman, Convection regime flow in a vertical slot: Continuum of solutions from capped to open ends, Heat Mass Transf. 43(2006), 103-109.

[22] P.D. Weidman and A. Medina, Porous media convection between vertical walls: Continuum of solutions from capped to open ends, Acta Mech., 199(2008), 209-216.
[23] P.J. Prescott and F.P. Incropera, Magnetically damped convection during solidification of a binary metal alloy, J. Heat Transfer, 115(1993), 302-310.
[24] R. Kandasamy, I. Muhaimin and A.B. Khami's, Thermophoresis and variable viscosity effects on MHD mixed convective heat and mass transfer past a porous wedge in the presence of chemical reaction, Heat Mass Transfer, 45(2009), 703-712.
[25] R. Siegel and J.R. Howell, Thermal Radiation Heat Transfer, International Student Edition, Mc Graw-Hill, New York, 1972.
[26] S. Alchaar, P. Vasseur and E. Bilgen, Hydromagnetic natural convection in a tilted rectangular porous enclosure, Numer. Heat transfer A, 27(1995), 107-127.
[27] S.H. Kim, N.K. Anand and W. Aung, Effect of wall conduction on free convection between asymmetrically heated vertical plates, Uniform wall heat flux, Int. J. Heat Mass Transfer, 33(1990), 1013-1023.
[28] T. Burch, T. Rhodes and S. Acharya, Laminar natural convection between finitely conducting vertical plates, Int. J. Heat Mass Transfer, 28(1985), 1173-1186.
[29] T.G. Cowling, Magnetohydrodynamics, Interscience Publishers, N.Y., 1957.
[30] T. Hayat, M. Javed and N. Ali, MHD peristaltic transport of a Jeffery fluid in a channel with compliant walls and porous space, Trans. Porous Media, 74(2008), 259-274.
[31] V.R. Prasad and N.B. Reddy, Radiation effects on an unsteady MHD convective heat and mass transfer flow past a semi-infinite vertical permeable moving plate embedded in a porous medium, J. Energy, Heat and Mass Transfer, 30(2008), 57-78.
[32] W. Aung, L.S. Fletcher, and V. Sernas, Developing laminar free convection between vertical flat plates with asymmetric heating, Int. J. Heat Mass Transf., 15(1972), 2293-2304.
[33] W. Bian, P. Vasseur, E. Bilgen and F. Meng, Effect of an electromagnetic field on natural convection in an inclined porous layer, Int. J. Heat Fluid Flow, 17(1996), 36-44.
[34] W.J. Chang and W.L. Chang, Mixed convection in a vertical parallel plate channel partially filled with porous media of high permeability, Int. J. Heat Mass Transf., 39(1996), 1331-1342.

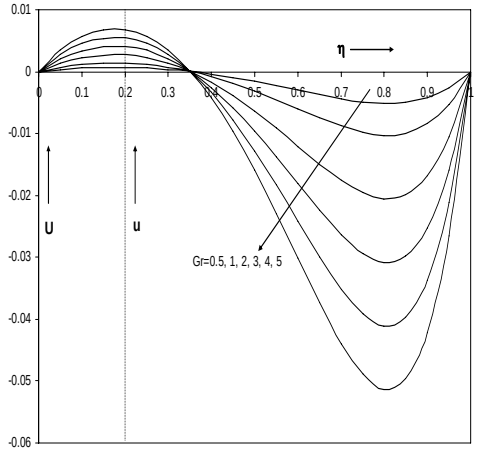

Fig.2 Velocity profiles in x- direction U, u vs η for K=0.1, M^2=2, N=1, Pr=7, Re=9, n=0.2, t=1, $\lambda = 1$, $\varepsilon = 0.1$.

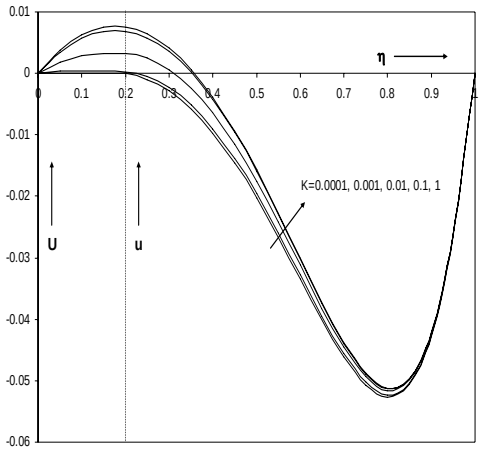

Fig.3 Velocity profiles in x- direction U, u vs η for Gr=5, M^2=2, N=1, Pr=7, Re=9, n=0.2, t=1, $\lambda = 1$, $\varepsilon = 0.1$.

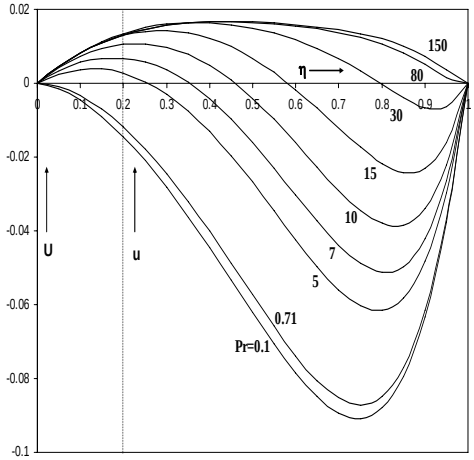

Fig.4 Velocity profiles in x- direction U, u vs η for Gr=5, K=0.1, M^2=2, N=1, Re=9, n=0.2, t=1, $\lambda = 1, \varepsilon = 0.1.$

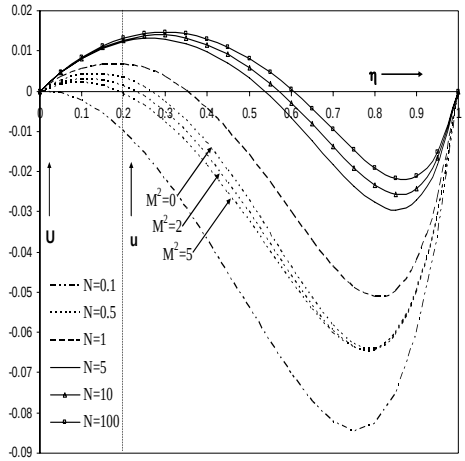

Fig.5 Velocity profiles in x- direction U, u vs η for Gr=5, K=0.1, M^2=2, Pr=7, Re=9, n=0.2, t=1, $\lambda = 1, \varepsilon = 0.1.$

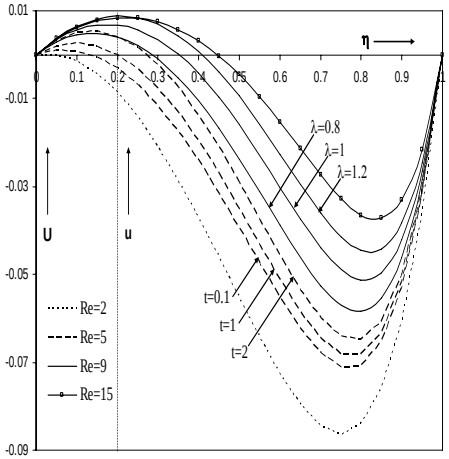

Fig.6 Velocity profiles in x- direction U, u vs η for Gr=5, K=0.1, M^2=2, N=1, Pr=7, n=0.2, t=1, $\lambda = 1, \varepsilon = 0.1.$

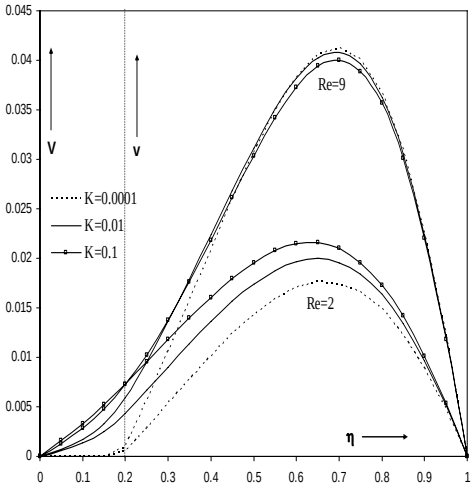

Fig.7 Velocity profiles in y- direction V, v vs η for Gr=5, M^2=2, N=1, Pr=7, Re=9, n=0.2, t=1, $\lambda = 1, \varepsilon = 0.1.$

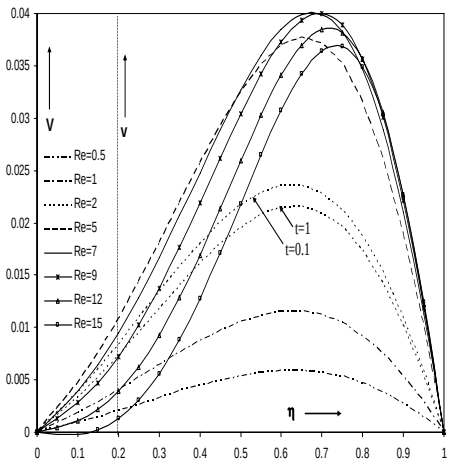

Fig.8 Velocity profiles in y- direction V, v vs η for Gr=5, K=0.1, M^2=2, N=1, Pr=7, n=0.2, t=1, $\lambda = 1, \varepsilon = 0.1.$

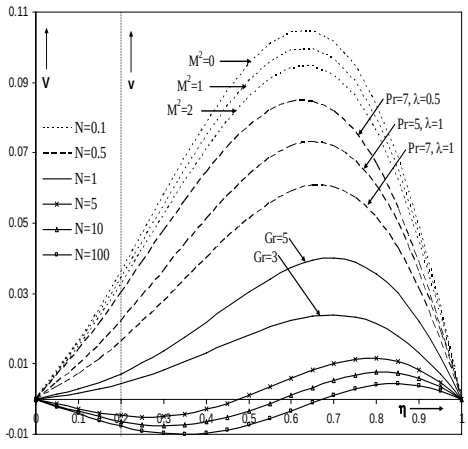

Fig.9 Velocity profiles in y- direction V, v vs η for Gr=5, K=0.1, M^2=2, Pr=7, Re=9, n=0.2, t=1, $\lambda = 1, \varepsilon = 0.1.$

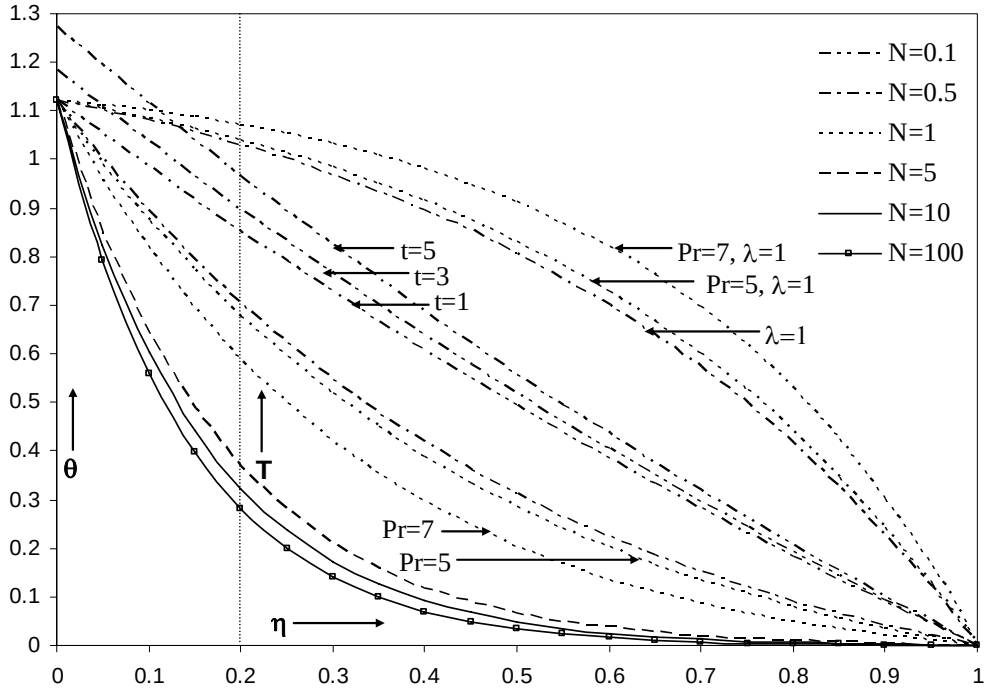

Fig.10 Temperature distribution θ, T vs η for Pr=7, n=0.2, t=1, $\lambda = -1$, $\varepsilon = 0.1$.

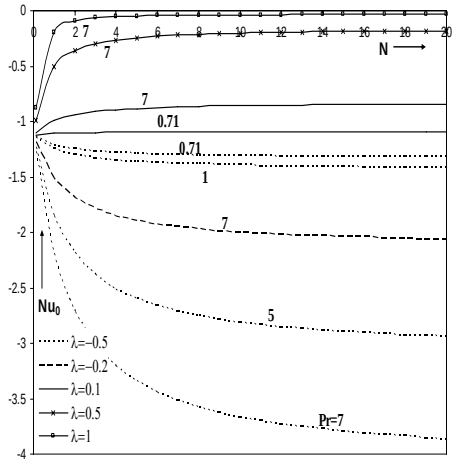

Fig.11 Nusselt number Nu_0 vs N for n=0.2, t=1, $\varepsilon = 0.1$.

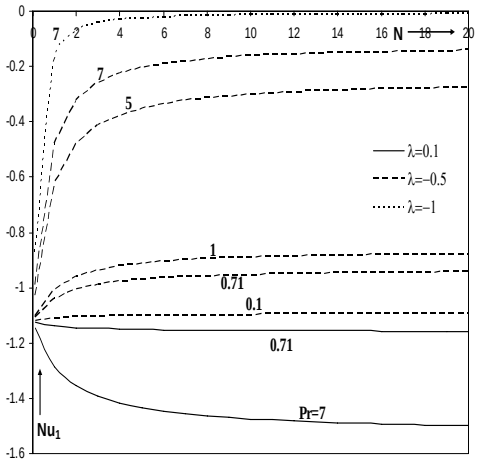

Fig.12 Nusselt number Nu_1 vs N for n=0.2, t=1, $\varepsilon = 0.1$.